ISSN 1674-1056
http://cpb.iphy.ac.cn
http://iopscience.iop.org/cpb
中国物理 B
Chinese Physics
中国物理 Chinese Physics B

Real-space observation on standing configurations of phenylacetylene on Cu (111) by scanning probe microscopy

Jing Qi(戚竞), Yi-Xuan Gao(高艺璇), Li Huang(黄立), Xiao Lin(林晓), Jia-Jia Dong(董佳家), Shi-Xuan Du(杜世萱), Hong-Jun Gao(高鸿钧)

Citation: Chin. Phys. B . 2019, 28(6): 066801. **doi:** 10.1088/1674-1056/28/6/066801
Journal homepage: http://cpb.iphy.ac.cn; http://iopscience.iop.org/cpb

What follows is a list of articles you may be interested in

Interaction of two symmetric monovacancy defects in graphene

Wen-Yan Xu(徐文焱), Li-Zhi Zhang(张礼智), Li Huang(黄立), Yan-De Que(阙炎德), Ye-Liang Wang(王业亮), Xiao Lin(林晓), Shi-Xuan Du(杜世萱)

Chin. Phys. B . 2019, 28(4): 046801. **doi:** 10.1088/1674-1056/28/4/046801

Domain boundaries in silicene: Density functional theory calculations on electronic properties

Xiao Hong-Jun, Zhang Li-Zhi, Du Shi-Xuan, Gao Hong-Jun

Chin. Phys. B . 2015, 24(8): 086806. **doi:** 10.1088/1674-1056/24/8/086806

Adsorption of glycine on diamond (001): Role of bond angle ofcarbon atoms

Li Lin, Xu Jing, Xu Li-Fang, Lian Chao-Sheng, Li Jun-Jie, Wang Jian-Tao, Gu Chang-Zhi

Chin. Phys. B . 2015, 24(5): 056803. **doi:** 10.1088/1674-1056/24/5/056803

Tensile properties of phase interfaces in Mg–Li alloy：A first principles study

Zhang Cai-Li, Han Pei-De, Wang Xiao-Hong, Zhang Zhu-Xia, Wang Li-Ping, Xu Hui-Xia

Chin. Phys. B . 2013, 22(12): 126802. **doi:** 10.1088/1674-1056/22/12/126802

First-principles study of Ar adsorptions on the (111) surfaces of Pd, Pt, Cu, and Rh

Niu Wen-Xia, Zhang Hong, Gong Min, Cheng Xin-Lu

Chin. Phys. B . 2013, 22(6): 066802. **doi:** 10.1088/1674-1056/22/6/066802

Real-space observation on standing configurations of phenylacetylene on Cu (111) by scanning probe microscopy*

Jing Qi(戚竞)[1], Yi-Xuan Gao(高艺璇)[1], Li Huang(黄立)[1,†], Xiao Lin(林晓)[1], Jia-Jia Dong(董佳家)[2], Shi-Xuan Du(杜世萱)[1,3,‡], and Hong-Jun Gao(高鸿钧)[1,3]

[1] *Institute of Physics & University of Chinese Academy of Sciences, Chinese Academy of Sciences, Beijing* 100190, *China*
[2] *Key Laboratory of Organofluorine Chemistry, Center for Excellence in Molecular Synthesis, Shanghai Institute of Organic Chemistry, Chinese Academy of Sciences, Shanghai* 200032, *China*
[3] *Beijing Key Laboratory for Nanomaterials and Nanodevices, Beijing* 100190, *China*

(Received 11 March 2019; revised manuscript received 4 April 2019; published online 8 May 2019)

The adsorption configurations of molecules adsorbed on substrates can significantly affect their physical and chemical properties. A standing configuration can be difficult to determine by traditional techniques, such as scanning tunneling microscopy (STM) due to the superposition of electronic states. In this paper, we report the real-space observation of the standing adsorption configuration of phenylacetylene on Cu (111) by non-contact atomic force microscopy (nc-AFM). Deposition of phenylacetylene at 25 K shows featureless bright spots in STM images. Using nc-AFM, the line features representing the C–H and C–C bonds in benzene rings are evident, which implies a standing adsorption configuration. Further density functional theory (DFT) calculations reveal multiple optimized adsorption configurations with phenylacetylene breaking its acetylenic bond and forming C–Cu bond(s) with the underlying copper atoms, and hence stand on the substrate. By comparing the nc-AFM simulations with the experimental observation, we identify the standing adsorption configuration of phenylacetylene on Cu (111). Our work demonstrates an application of combining nc-AFM measurements and DFT calculations to the study of standing molecules on substrates, which enriches our knowledge of the adsorption behaviors of small molecules on solid surfaces at low temperatures.

Keywords: phenylacetylene, adsorption configuration, scanning probe microscopy, density functional theory

PACS: 68.43.–h, 68.43.Fg, 07.79.–v, 31.15.E **DOI:** 10.1088/1674-1056/28/6/066801

1. Introduction

Adsorption configurations can significantly affect the physical and chemical properties of molecules adsorbed on substrates, such as self-assembly[1–4] and catalytic activity.[5–7] Studying the adsorption configurations of molecules on substrates can not only help us understand molecule–substrate interactions,[4,8–12] but will also enable us to tailor molecules' properties,[13–15] which will ultimately pave the way for molecular devices.[16–18] Spectroscopies have been widely used for their ability to distinguish the electronic structural changes of different adsorption configurations of a molecule but can hardly allow any real-space observation.[19,20] Scanning tunneling microscopy (STM) is a powerful tool that is widely used to implement the real-space observation of molecules.[21] However, for standing molecules, using STM to determine their adsorption configurations can be a great challenge[16,22–26] due to the superposition of electronic states. Meanwhile, non-contact atomic force microscopy (nc-AFM) allow the clear imaging of the topmost chemical bonds in standing molecules[16] due to its ability to detect atomic force.[27–32] Therefore, unambiguous identification of the adsorption configuration of standing molecules can be achieved by combining nc-AFM with density functional theory (DFT) calculations.

Phenylacetylene (PA, C_8H_6) consists of an alkyne group bonded to a benzene ring. Prior spectroscopic studies showed that the acetylenic bond in PA has a strong interaction with a copper surface, hence PA exhibits standing adsorption configuration on copper substrate.[33,34] However, real space observations have been limited.[35] Here, we report that the real-space observation and identification of the standing adsorption configuration of PA on Cu (111) through nc-AFM. STM measurements yield featureless bright spots after deposition of PA at 25 K. However, the nc-AFM measurements yield evident line features representing the chemical bonds, implying a standing adsorption configuration. With the help of DFT calculations, several optimized adsorption configurations are found with PA breaking its acetylenic bond and forming C–Cu bond(s) with the underlying copper atoms, and hence stand on substrate. By comparing structural features in nc-AFM

*Project supported by the National Key Research and Development Program of China (Grant Nos. 2016YFA0202300 and 2018YFA0305800), the National Natural Science Foundation of China (Grant Nos. 61888102, 61474141, and 21661132006), the Young Scientists Fund of the National Natural Science Foundation of China (Grant No. 11604373), the Outstanding Youth Science Foundation, China (Grant No. 61622116), and the Strategic Priority Research Program of Chinese Academy of Sciences (CAS) (Grant Nos. XDB28000000 and XDB30000000).

†Corresponding author. E-mail: lhuang@iphy.ac.cn
‡Corresponding author. E-mail: sxdu@iphy.ac.cn

© 2019 Chinese Physical Society and IOP Publishing Ltd

measurements and corresponding simulations, we identify the standing adsorption configuration of PA on Cu (111).

2. Methods

2.1. Experimental techniques

Our experiments were accomplished in an ultra-high vacuum (UHV) STM/nc-AFM system at liquid helium (LHe) temperature with the base pressure better than 2×10^{-10} mbar (1 bar = 10^5 Pa). Single-crystal Cu (111) surface was prepared in a UHV chamber by repeated circles of Ar^+ ion sputtering and subsequent annealing at 660 K for 20 min. Commercial PA molecules (Sigma-Aldrich, 98%) were degassed by repeated freeze–pump–thaw cycles. The PA was then evaporated at room temperature (RT) in gaseous phase onto a clean Cu (111) surface *in situ* through a leak valve in UHV chamber while keeping the Cu (111) substrate under 25 K all the time. The evaporation pressure was 8.0×10^{-10} mbar and evaporation time was controlled between 0.8 s–5 s. The Cu (111) sample was transferred into STM head and cooled down to LHe temperature the moment that PA evaporation was finished. All STM topographic images were acquired in a constant-current mode. All nc-AFM measurements were performed by using a commercial qPlus tuning fork sensor in the frequency modulation mode with a CO-terminated Pt/Ir tip.[36] The resonance frequency was about 27.9 kHz, and stiffness about 1800 N/m. The imaging heights for all nc-AFM measurements reported throughout the text referred to the STM tunneling junction height on a clean Cu (111) substrate. All STM and nc-AFM images were processed by using the Gwyddion free and open source software program.

2.2. Computational methods

All of our calculations were carried out within density functional theory by using Vienna *ab initio* simulation package (VASP).[37] The projector augmented wave (PAW) method[38] was employed. A generalized gradient approximation (GGA) in the form of Perdew–Burke–Ernzerhof (PBE) was adopted for the exchange–correlation functional.[39] The electronic wave functions were expanded in plane waves with a kinetic energy cutoff of 400 eV. The k-points' mesh used in the calculations was $1 \times 1 \times 1$ due to the large dimension of simulation supercell. The k-points mesh and other parameters were tested. A slab model was used with three Cu layers serving as the substrate. The thickness of vacuum layer was larger than 2 nm. All atoms but for those in the bottom Cu layer were fully relaxed until the residual forces were smaller than 0.1 eV/nm.

To simulate the high-resolution AFM images, we used a mechanical probe-particle AFM model in which the CO molecule at the tip was considered as a spherical particle.[40] The following parameters were used for the probe-particle model: the effective lateral stiffness of the CO molecule $k = 0.5$ N·m^{-1} and the oscillation amplitude $A_{\mathrm{osc}} = 0.2$ nm. The molecular structures were obtained from the DFT calculations.

3. Results and discussion

The PA molecules are evaporated onto clean Cu (111) substrates in gaseous phase for STM and nc-AFM measurements. To improve the STM image resolution and nc-AFM measurements, carbon monoxide (CO) is dosed onto Cu (111) substrate at LHe temperature. Figure 1 shows the STM topographic images of PA evaporated on Cu (111) substrate at LHe temperature, and a typical monomer and dimer using a CO functionalized tip.[36] Figure 1(a) shows a large-scaled STM image, and the PA coverage is about 0.07/nm^2. When evaporated onto a clean Cu (111) substrate, PA molecules are mostly adsorbed as isolated monomers with a few dimers. Figures 1(b) and 1(c) show a typical PA monomer and dimer, respectively. The line profile across the monomer along the blue arrow in Fig. 1(b) and across the dimer along the red arrow in Fig. 1(c) are shown, respectively, in the upper and lower part of Fig. 1(d), indicating that the typical STM height of a PA molecule adsorbed on Cu (111) is about 0.22 nm. Each PA molecule appears as a bright circular protrusion surrounded by a dimmer periphery. Judging from its height and symmetry, we can infer that PA molecules adsorbed on Cu (111) have a standing configuration rather than a flat or tilting configuration. The STM topography of PA molecules is almost circularly

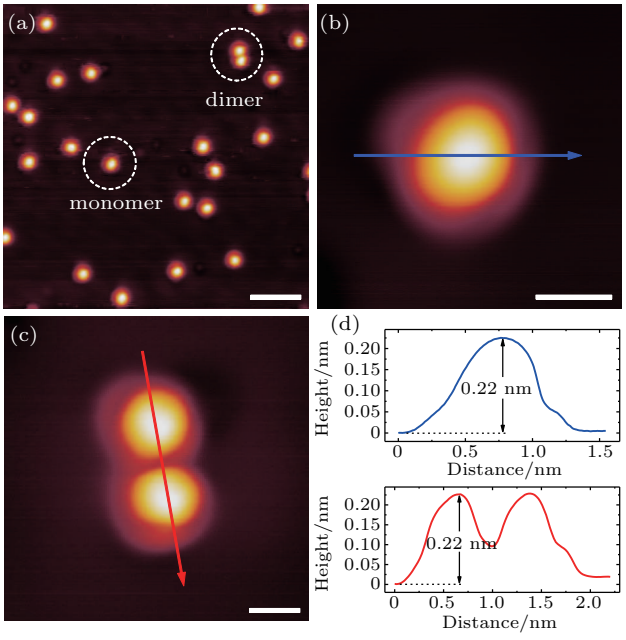


Fig. 1. STM imaging of PA on Cu (111) substrate. (a) STM topography of PA molecules on Cu (111) substrate at LHe temperature. Dashed circles indicate typical PA monomer and dimer. Scale bar: 3 nm. (b) High-resolution STM image of PA monomer. Scale bar: 0.5 nm. (c) High-resolution STM image of PA dimer. Scale bar: 0.5 nm. (d) Line profile across monomer along blue arrow in panel 1(b) and the dimer along the red arrow in panel 1(c). STM scanning parameters: $V_{\mathrm{Sample}} = -100$ mV and $I = 50$ pA.

symmetric without any detailed resolution of the standing benzene ring due to the superposition of electronic states.

Figure 2 shows the AFM measurements of a PA monomer and dimer on Cu (111) substrate. Figure 2(a) displays the STM topography of a PA monomer. The molecular structure of PA is superposed on the top, and the topmost hydrogen atom is denoted as H1. Figures 2(b)–2(d) show the corresponding nc-AFM images. At higher imaging heights, we first observe a bright spot in Fig. 2(b). When the tip gets closer, we can see a bright line feature marked by red arrow "I" and a vague line feature marked by red arrow "II" in Fig. 2(c). At even lower imaging height, another vague line feature appears as marked by red arrow "III" in Fig. 2(d), and the line features "I" and "II" appear even brighter. To understand the evolutions of the nc-AFM images at different imaging heights, we assume that the PA molecule is standing on the substrate with its acetylene bonding to the substrate and the plane of benzene ring almost vertical to the substrate. Therefore, at the higher imaging height, the topmost hydrogen atom (the H1 in Fig. 2(a)) enters into the distance of force interaction with the tip and therefore appears as a bright spot in Fig. 2(b). When the tip gets closer, the topmost C–H bond in PA's benzene ring starts to get involved and appears as a bright line feature marked by red arrow "I". Meanwhile, one of the C–C bonds connecting the topmost C atom marked by red arrow "II" shows a vague line feature. At even lower imaging height, the other C–C bond connecting the topmost C atom in the benzene ring becomes distinct as marked by red arrow "III". Figure 2(e) shows the STM topography of a PA dimer, and figures 2(f)–2(h) display the corresponding nc-AFM images. Similarly, line features representing the topmost C–H bonds (I_a, I_b) and the C–C bonds (II_a, II_b, III_a, III_b) are distinct as marked by red arrows in Fig. 2(h). These results clearly infer an upright benzene ring and a standing adsorption configuration of PA adsorbed on Cu (111) substrate.

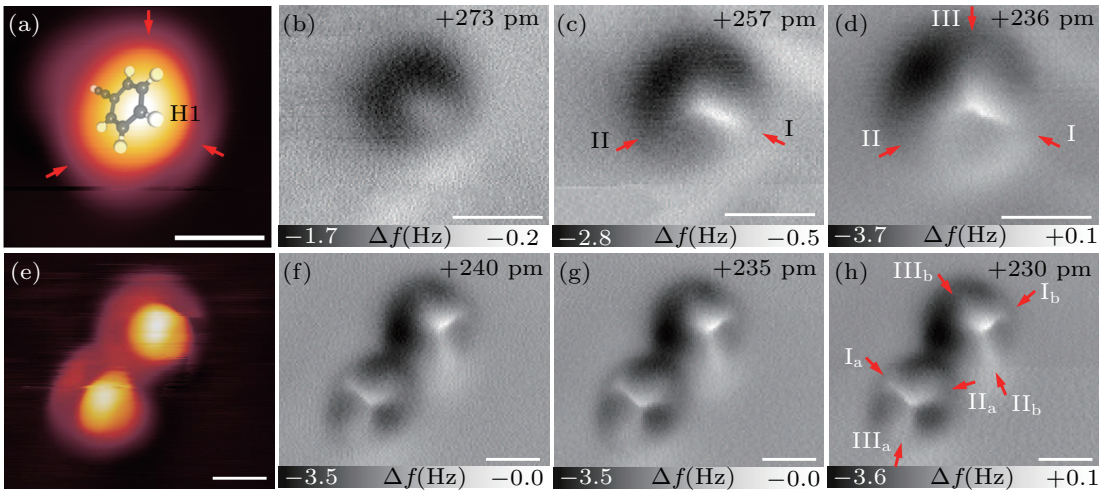


Fig. 2. STM and constant-height nc-AFM images of PA monomer and dimer on Cu (111) substrate. (a) STM topography of PA monomer. Molecular structure of PA is superposed on top, and the topmost hydrogen atom is denoted as H1. (b)–(d) Corresponding nc-AFM images of PA monomer in Fig. 2(a) at different imaging heights. AFM imaging height refers to tunneling junction height and marked on top right of each AFM image. Red arrows indicate bright line features of PA monomer. (e) STM topography of PA dimer. (f)–(h) Corresponding nc-AFM images of PA dimer in panel (e) at different imaging heights. Red arrows indicate the bright line features of PA dimer. STM scanning parameters: $V_{\text{Sample}} = -100$ mV and $I = 50$ pA. Scale bars: 0.5 nm.

To verify our speculations and obtain the exact adsorption configuration of PA on Cu (111) substrate, we then carry out DFT calculations for comparison with nc-AFM measurements. We construct two groups of standing configurations with PA molecules chemisorbed on the Cu (111) substrate. The PA molecule in one group sits on the substrate with the terminal C1 atom bonding to the substrate, while that in the other group bonds to the substrate with acetylene as shown in Fig. 3. The adsorption of PA molecules in the first group involves tautomerization of the ethyne group, with the proton moving to the C2 position (as shown in Fig. 3(a)) to form a Cu-bonded phenylvinylidene. We consider two adsorption sites marked as black balls for group-one molecules and four sites marked as black dumbbells for group-two molecules as shown in Fig. 3(b). We finally obtain two configurations shown in Figs. 3(c) and 3(d). We also calculate the adsorption energy (E_{ad}) of these two configurations, which is defined as $E_{\text{ad}} = E_{\text{tot}} - E_{\text{Cu}} - E_{\text{PA}}$. The E_{tot}, E_{Cu}, and E_{PA} are the energy values of the relaxed PA–on–Cu (111) system, relaxed Cu substrate and relaxed PA molecule, respectively. The values of adsorption energy are -1.272 eV and −1.434 eV for the configurations in Fig. 3(c) and 3(d), respectively. The styrene derivative configuration gives a much lower value of adsorption energy (−1.434 eV) than the phenylvinylidene configuration (−1.272 eV), which means that it is more energy-preferable on Cu (111) substrate.

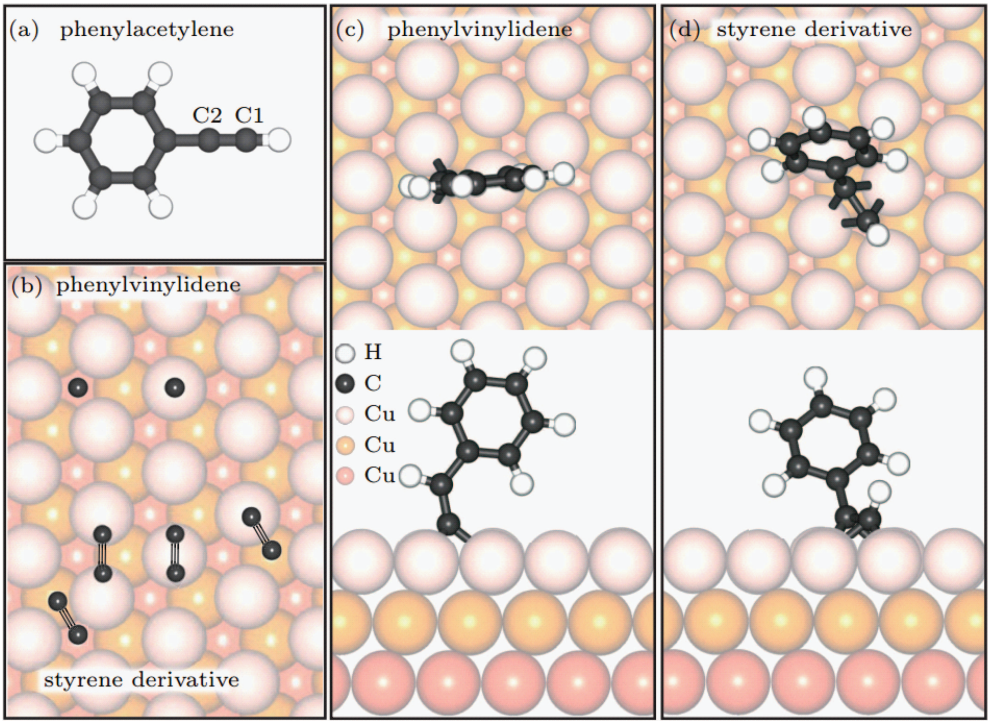


Fig. 3. DFT optimized adsorption configurations of PA on Cu (111). (a) schematic representation of PA, and two carbon atoms in the acetylenic bond are denoted as C1 and C2. (b) Initial adsorption positions considered in DFT calculations. The black balls indicate the C1 positions in phenylvinylidene form, and black dumbbells refer to the C1–C2 bond positions in styrene derivative form. All of the initial adsorption configurations are optimized into two final configurations as shown in panels (c) and (d). (c) and (d) DFT optimized phenylvinylidene model and styrene derivative model, respectively.

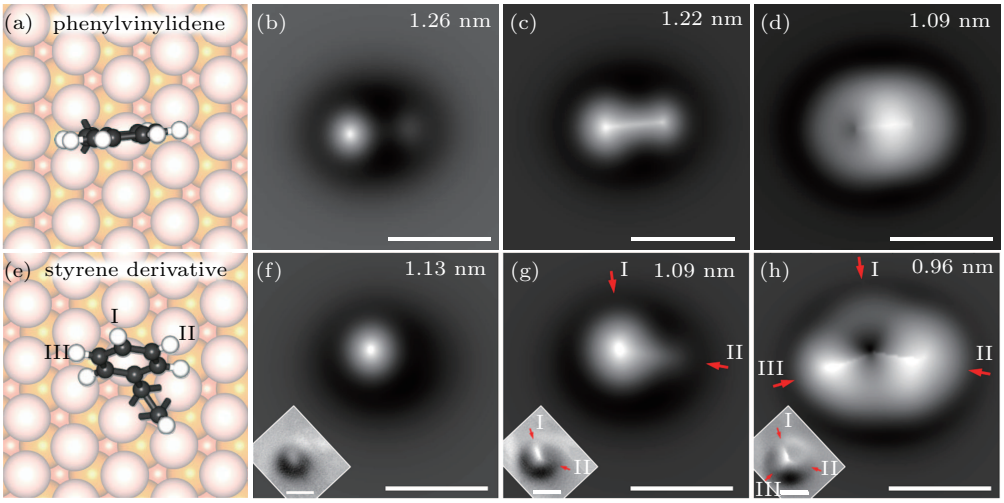


Fig. 4. AFM simulations of PA on Cu (111) substrate. (a) Phenylvinylidene model and (b)–(d) its corresponding AFM simulations at different imaging heights. (e) Styrene derivative model and (f)–(h) its corresponding AFM simulations at different imaging heights. Heights used in calculations are marked on the top right of each simulated image. Scale bars: 0.5 nm. Insets in panels (f)–(h) used for comparison show experimental nc-AFM images in Figs. 2(b)–2(d), respectively.

We simulate the nc-AFM images based on these two configurations. Figures 4(a)–4(d) show the phenylvinylidene model and the corresponding nc-AFM simulations as the tip approaches to the surface. In these images, the features that first appear are two spots with different brightness as shown in Fig. 4(b), representing the two topmost C–H bonds that have a slight height difference (referring to the lower panel in Fig. 3(c)). When the tip gets closer, a bright line feature emerges and connects the bright spots (Fig. 4(c)), which corresponds to the topmost C–C bond in the benzene ring. With an even smaller imaging height, the feature extends into an oval, as shown in Fig. 4(d). We note that the features are not consistent with those of the AFM images in Fig. 2.

Figures 4(e)–4(h) are the styrene derivative model and the corresponding nc-AFM simulations with decreasing imaging heights. For comparison, the nc-AFM experimental images are shown with insets in simulated AFM images in Figs. 4(f)–4(h), and rotated to the same directions as those in the sim-

ulations. The topmost C–H bond and the two adjacent C–C bonds are marked as "I", "II" and "III" as shown in Fig. 4(e). In Fig. 4(f), the bright spot feature originates from "I" and dark halo to the bottom right both fit to each other perfectly in the experimental and simulated images. At a lower imaging height in Fig. 4(g), the bright features caused by "I" and "II" both accord well with the experimental image in the inset, except for the fact that the shape of the feature "I" is an oval rather than a line in simulation. When the imaging height further decreases in Fig. 4(h), another line feature arises on the left-hand side, making the simulated image have a three-feature layout in the same way as in the experimental image, only the feature "I" is dark. We note that the two differences between experiment and simulation are both related to the topmost C–H bond (feature "I"). These two differences can be explained as follows. In the AFM simulations, the PA molecule is fixed, which makes the C–H bond shadowed by its top hydrogen atom during imaging. Therefore, the topmost H atom blocks the feature of C–H bond and yields the bright oval feature for "I" in Fig. 4(g). For the same reason, when the tip height decreases further, the interaction force of the tip with the topmost C–H bond enters into the deep repulsive regime, which leads it to appear as a dark feature in Fig. 4(h). However, in experiment, it is highly possible that the benzene ring is pushed down to a certain extent by the tip during measurements,[40,41] which makes it impossible for the topmost C–H bond to enter into the deep repulsive region and should also be the reason why we can see three bright line features in experimental images. Overall, the simulation based on the styrene derivative model accords well with the nc-AFM images.

4. Conclusions

Using STM and nc-AFM as a powerful tool to verify our DFT calculated model, we study the adsorption configurations of PA molecules on Cu (111) substrate at LHe temperature. STM measurements yield featureless bright spots after deposition of PA. However, the nc-AFM measurements yield evident line features representing the chemical bonds, which implies a standing adsorption configuration. By comparing nc-AFM results with AFM simulations, we identify the adsorption configuration of PA on Cu (111) as a styrene derivative. Our work demonstrates an application of combining nc-AFM measurements and DFT calculation to the study of standing molecules on substrates, which enriches our knowledge of the adsorption behaviors small molecules on solid surfaces at low temperatures.

Acknowledgment

Part of the research was performed in the Key Laboratory of Vacuum Physics, Chinese Academy of Sciences. Computational resources were provided by the National Supercomputing Center in Tianjin Municipality, China.

References

[1] Giancarlo L C, Fang H B, Rubin S M, Bront A A and Flynn G W 1998 *J. Phys. Chem. B* **102** 10255
[2] Kirakosian A, Comstock M J, Cho J and Crommie M F 2005 *Phys. Rev. B* **71** 113409
[3] Ramoino L, von Arx M, Schintke S, Baratoff A, Guntherodt H J and Jung T A 2006 *Chem. Phys. Lett.* **417** 22
[4] Du S X, Gao H J, Seidel C, Tsetseris L, Ji W, Kopf H, Chi L F, Fuchs H, Pennycook S J and Pantelides S T 2006 *Phys. Rev. Lett.* **97** 156105
[5] Zaera F 2002 *Surf. Sci.* **500** 947
[6] Somorjai G A and Yang M C 2003 *Top. Catal* **24** 61
[7] Deng X Y, Min B K, Guloy A and Friend C M 2005 *J. Am. Chem. Soc.* **127** 9267
[8] Velic D, Hotzel A, Wolf M and Ertl G 1998 *J. Chem. Phys.* **109** 9155
[9] Schroeder P G, France C B, Park J B and Parkinson B A 2002 *J. Appl. Phys.* **91** 3010
[10] Huang W X and White J M 2004 *J. Phys. Chem. B* **108** 5060
[11] Shi D, Ji W, Lin X, He X, Lian J, Gao L, Cai J, Lin H, Du S, Lin F, Seidel C, Chi L, Hofer W, Fuchs H and Gao H J 2006 *Phys. Rev. Lett.* **96** 226101
[12] Li N, Huang Y, Du F, He X B, Lin X, Gao H J, Ma Y F, Li F F, Chen Y S and Eklund P C 2006 *Nano Lett.* **6** 1141
[13] Gao L, Ji W, Hu Y B, Cheng Z H, Deng Z T, Liu Q, Jiang N, Lin X, Guo W, Du S X, Hofer W A, Xie X C and Gao H J 2007 *Phys. Rev. Lett.* **99** 106402
[14] Gao L, Liu Q, Zhang Y Y, Jiang N, Zhang H G, Cheng Z H, Qiu W F, Du S X, Liu Y Q, Hofer W A and Gao H J 2008 *Phys. Rev. Lett.* **101** 197209
[15] Zhang H G, Mao J H, Liu Q, Jiang N, Zhou H T, Guo H M, Shi D X and Gao H J 2010 *Chin. Phys. B* **19** 018105
[16] Esat T, Friedrich N, Tautz F S and Temirov R 2018 *Nature* **558** 573
[17] Schliwa M and Woehlke G 2003 *Nature* **422** 759
[18] Hu Y B, Zhu Y, Gao H J and Guo H 2005 *Phys. Rev. Lett.* **95** 156803
[19] Stöhr J 1992 *NEXAFS Spectroscopy* (Berlin, Heidelberg: Springer-Verlag)
[20] Hofmann S 2013 *Auger- and X-Ray Photoelectron Spectroscopy in Materials Science* (Berlin, Heidelberg: Springer-Verlag)
[21] Gimzewski J K and Joachim C 1999 *Science* **283** 1683
[22] Larson A M, van Baren J, Kintigh J, Wang J, Tang J M , Zahl P, Miller G P and Pohl K 2018 *J. Phys. Chem. C* **122** 11938
[23] Vernisse L, Guillermet O, Gourdon A and Coratger R 2018 *Surf. Sci.* **669** 87
[24] Peng J B, Guo J, Hapala P, Cao D Y, Ma R Z, Cheng B W, Xu L M, Ondracek M, Jelinek P, Wang E G and Jiang Y 2018 *Nat. Commun.* **9** 122
[25] Moreno C, Stetsovych O, Shimizu T K and Custance O 2015 *Nano Lett.* **15** 2257
[26] Albrecht F, Pavlicek N, Herranz-Lancho C, Ruben M and Repp J 2015 *J. Am. Chem. Soc.* **137** 7424
[27] Gross L, Mohn F, Moll N, Schuler B, Criado A, Guitian E, Pena D, Gourdon A and Meyer G 2012 *Science* **337** 1326
[28] Gross L, Mohn F, Moll N, Liljeroth P and Meyer G 2009 *Science* **325** 1110
[29] Pavlicek N, Fleury B, Neu M, Niedenfuhr J, Herranz-Lancho C, Ruben M and Repp J 2012 *Phys. Rev. Lett.* **108** 086101
[30] Zhang J, Chen P C, Yuan B K, Ji W, Cheng Z H and Qiu X H 2013 *Science* **342** 611
[31] Gross L, Mohn F, Moll N, Meyer G, Ebel R, Abdel-Mageed W M and Jaspars M 2010 *Nat. Chem.* **2** 821
[32] Giessibl F J 2003 *Rev. Mod. Phys.* **75** 949
[33] Iucci G, Carravetta V, Altamura P, Russo M V, Paolucci G, Goldoni A and Polzonetti G 2004 *Chem. Phys.* **302** 43
[34] Sohn Y, Wei W and White J M 2007 *J. Phys. Chem. C* **111** 5101
[35] Li Q, Han C B, Fuentes-Cabrera M, Terrones H, Sumpter B G, Lu W C, Bernholc J, Yi J Y, Gai Z, Baddorf A P, Maksymovych P and Pan M H 2012 *ACS Nano* **6** 9267
[36] Bartels L, Meyer G and Rieder K H 1997 *Appl. Phys. Lett.* **71** 213
[37] Kresse G and Furthmuller J 1996 *Phys. Rev. B* **54** 11169
[38] Blochl P E 1994 *Phys. Rev. B* **50** 17953
[39] Perdew J P, Burke K and Ernzerhof M 1996 *Phys. Rev. Lett.* **77** 3865
[40] Hapala P, Kichin G, Wagner C, Tautz F S, Temirov R and Jelinek P 2014 *Phys. Rev. B* **90** 085421
[41] Shiotari A, Odani T and Sugimoto Y 2018 *Phys. Rev. Lett.* **121** 116101